MOLECULAR PHARMACOLOGY, 19:367–371

Mathematical Analysis of the Kinetics of Competitive Inhibition in Neurotransmitter Receptor Binding Assays

FREDERICK J. EHLERT, WILLIAM R. ROESKE,[1] AND HENRY I. YAMAMURA[2]

Departments of Pharmacology, Psychiatry, and Internal Medicine, University of Arizona Health Sciences Center, Tucson, Arizona 85724

Received June 30, 1980; Accepted December 29, 1980

SUMMARY

EHLERT, F. J., W. R. ROESKE, AND H. I. YAMAMURA. Mathematical analysis of the kinetics of competitive inhibition in neurotransmitter receptor binding assays. *Mol. Pharmacol.* 19:367–371 (1981).

The kinetics of competitive inhibition was described by first-order differential equations, and the solution to these equations was derived numerically. The results of this analysis showed that the IC_{50} of a competitive inhibition curve decreases as equilibrium is approached if the dissociation rate constant of the nonlabeled ligand is equal to or less than that of the labeled ligand. The converse was true for competitive inhibition curves of a nonlabeled inhibitor with a dissociation rate constant greater than that of the labeled ligand. Nonequilibrium competitive inhibition experiments were performed using the muscarinic antagonist and agonist ligands, [^{3}H]quinuclidinyl benzilate and [^{3}H]*cis*-methyldioxolane, and results consistent with the theoretical predictions were observed.

INTRODUCTION

The mathematical theory for the kinetics of drug-receptor interactions and RIA[3] has been developed by several investigators (1–3). However, no extensive study of the kinetics of competitive inhibition in neurotransmitter receptor binding assays has been described. The conditions for such binding assays often involve competition between radiolabeled and nonlabeled drugs having different affinities. These conditions are uncommon in RIA experiments in which competition between the same labeled and nonlabeled ligand usually occurs. The kinetics of competitive inhibition in RIA, for competition between ligands having the same affinity, has been described by Rodbard *et al.* (4).

In the present report, we have described the kinetics of competitive inhibition in terms of first-order differential equations and have used computer simulation techniques to predict the shape of a competitive inhibition curve under nonequilibrium conditions. This analysis shows that the IC_{50} of a competitive inhibitor changes as equilibrium is approached. The direction of the change in IC_{50} is dependent upon the ratio of dissociation rate constants (k_{-1}/k_{-2}) of the two competing ligands. A recent mathematical analysis by Aranyi (5), describing the kinetics of competitive inhibition of ligands having different affinities, is consistent with the theoretical results of the present study. We have also performed nonequilibrium competitive inhibition experiments using the specific muscarinic agonist and antagonist affinity labels, [^{3}H]CD and [^{3}H]QNB, and have obtained binding data which are generally consistent with the computer simultation analysis. The results of our analysis are not intuitively obvious and suggest caution in designing and interpreting competitive inhibition experiments.

This work was supported in part by United States Public Health Service Grants MH-27257, MH-30626, and HL-21486 and by Program Project Grant HL-20984.

[1] Recipient of United States Public Health Service Research Scientist Development Award HL-00776 from the National Heart, Lung and Blood Institute.

[2] Recipient of United States Public Health Service Research Scientist Development Award MH-00095 (Type II) from the National Institute of Mental Health.

[3] The abbreviations used are: RIA, radioimmunoassay; [^{3}H]CD, [^{3}H]*cis*-methyldioxolane; [^{3}H]QNB, [^{3}H]quinuclidinyl benzilate.

METHODS

Kinetic theory of competitive inhibition. In the following analysis a simple bimolecular interaction of radiolabeled ligand (X) and competitive inhibitor (I) with the receptor (R) is assumed:

$$X + R \underset{k_{-1}}{\overset{k_1}{\rightleftharpoons}} XR \qquad (1)$$

$$I + R \underset{k_{-2}}{\overset{k_2}{\rightleftharpoons}} IR \qquad (2)$$

where k_1, k_{-1}, k_2, and k_{-2} are the reaction constants whereas XR and IR are ligand receptor complexes for X and I, respectively. Equations 1 and 2 give rise to the

0026-895X/81/030367-05$02.00/0

familiar equilibrium expressions:

$$K_x = k_{-1}/k_1 = [X][R]/[XR] \quad (3)$$

$$K_i = k_{-2}/k_2 = [I][R]/[IR] \quad (4)$$

where K_x and K_i are the equilibrium dissociation constants of X and I. Equations 3 and 4 can be solved analytically to give an equation which expresses the amount of X bound at equilibrium in the presence of the competitive inhibitor I:

$$[XR] = [X][R_T]/[X] + K_x(1 + [I]/K_i) \quad (5)$$

$$[R_T] = [R] + [XR] + [IR] \quad (6)$$

The net rates at which ligand receptor complexes form are given by the following differential equations:

$$d[XR]/dt = k_1[X][R] - k_{-1}[XR] \quad (7)$$

$$d[IR]/dt = k_2[I][R] - k_{-2}[IR] \quad (8)$$

The net rates at which the free ligand concentrations are depleted during the binding assay are given by the following differential equations:

$$d[X]/dt = -k_1[X][R] + k_{-1}[XR] \quad (9)$$

$$d[I]/dt = -k_2[I][R] + k_{-2}[IR] \quad (10)$$

The following conservation of mass equations also apply:

$$[X_T] = [X] + [XR] \quad (11)$$

$$[I_T] = [I] + [IR] \quad (12)$$

where $[X_T]$ and $[I_T]$ are the total concentrations of X and I. Equations 6–12 were solved numerically by Euler's method (6) so that theoretical competitive inhibition curves could be derived for nonequilibrium conditions. This procedure assumes that the rate of ligand binding is constant over a small time increment ($t_{i+1} - t_i$). This assumption allows the amount of ligand bound during the time increment to be calculated. The values of $[R]$, $[X]$ and $[I]$ are then readjusted by the conservation of mass equations (Eqs. 6, 11, and 12), and the process is repeated until equilibrium is reached ($d[XR]/dt = d[IR]/dt = 0$).

For a more precise description of this method, we can assume that Eqs. 7–10 are of the form

$$dy/dt = f(t, y) \quad (13)$$

To determine the free drug concentration or the amount of ligand bound (y) at any time point ($t_n = \sum_{i=1}^{n} t_i$), the following iteration is performed:

$$y_{i+1} = y_i + f(t_i, y_i)(t_{i+1} - t_i) \quad (14)$$

This iteration begins with initial conditions of $y_0 = 0$ and $t_0 = 0$. The initial values of the total drug and total receptor concentrations are given below. Note that Eq. 14 represents the first two terms in a Taylor's series expansion of y. By using a very small time interval ($t_{i+1} - t_i$) so that the derivatives are nearly constant over the interval, the computations are reasonably accurate if an adequate computer is used.

Binding assays. Rat forebrain homogenates were prepared from male Sprague-Dawley rats weighing 150–200 g. The forebrain (telencephalon and diencephalon) was homogenized in 10 volumes of 0.32 M sucrose with a Potter Elvehjem glass homogenizer and Teflon pestle. The crude homogenate was homogenized at 1,000 × *g* for 10 min and the pellet was discarded. The supernatant (S_1) was centrifuged at 17,500 × *g* for 20 min. This supernatant was discarded, and the pellet (P_2) was resuspended with a Polytron in 50 mM sodium-potassium-phosphate buffer, pH 7.4.

The specific binding of [^{3}H]QNB (29.4 Ci/mmole; New England Nuclear Corporation, Boston, Mass.) was determined according to the procedure of Yamamura and Synder (7) with minor modifications. In the standard assay, approximately 50 μg of protein of forebrain homogenate were incubated with 0.8 nM [^{3}H]QNB and various concentrations of competitive inhibitors in a final volume of 6 ml of 50 mM sodium-potassium-phosphate buffer, pH 7.4. Specific [^{3}H]QNB binding was calculated as total binding minus that occurring in the presence of 10 μM atropine. Incubations were carried out at 37° for the times indicated under Results.

[^{3}H]CD was custom-tritiated by Dr. Richard Young of New England Nuclear Corporation to a specific activity of 36.1 Ci/mmole. Specific [^{3}H]CD binding was measured essentially as described previously (8). Approximately 300 μg of protein of forebrain homogenate were incubated with 15 nM [^{3}H]CD and various concentrations of competitive inhibitors in a final volume of 2 ml containing 50 mM sodium-potassium-phosphate buffer. Assays were performed in triplicate, and specific binding was defined as the difference between measurements made in the presence and absence of 10 μM atropine. Incubations were carried out at 37° for the times indicated under Results. Following the incubations at 37°, the assay tubes were placed in an ice bath for 10 min. Subsequently the tubes were centrifuged at 27,000 × *g* for 10 min at 0°, and the supernatants were discarded. The pellets were superficially washed with two 3-ml aliquots of ice-cold 0.9% NaCl solution and solubilized with 300 μl of tissue solubilizer (NCS, Amersham/Searle Corporation, Arlington Heights, Ill.). The radioactivity of each sample was determined by liquid scintillation spectroscopy.

RESULTS

Theoretical predictions. Equilibrium and pre-equilibrium competitive inhibition curves were computed for the binding of a radiolabeled drug in the presence of various concentrations of a nonlabeled drug of equal or different affinity. For this analysis, the rate constants of the labeled drug were assigned values equal to those determined for [^{3}H]QNB in a previous report (9) ($k_1 = 1.03 \times 10^9$ M^{-1} min^{-1}, $k_{-1} = 2.45 \times 10^{-2}$ min^{-1}). In some instances, the value of k_{-1} was increased by a factor of 10. The total concentration of receptors was arbitrarily given a value of 2.5 pM. The rate constants (k_2, k_{-2}) of the nonlabeled drug were assigned values 10 times greater than, 10 times less than, and equal to the corresponding values of k_1 and k_{-1}. Theoretical competitive inhibition curves for all combinations of rate constants are shown in Fig. 1. When the dissociation rate constant of the nonlabeled drug was equal to or less than the dissociation rate constant of the radiolabeled drug, the competition

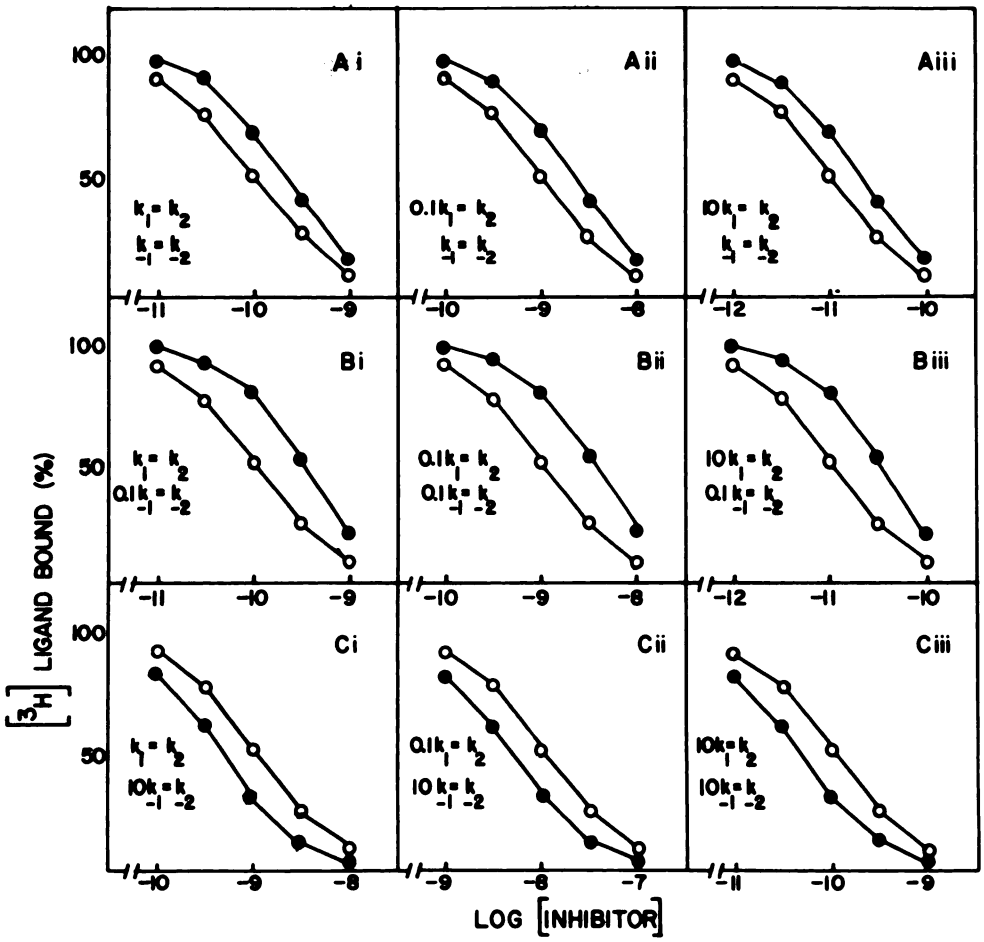

FIG. 1. *Kinetics of competitive inhibition*

Theoretical competitive inhibition curves were calculated numerically for pre-equilibrium (●) and equilibrium (○) conditions, corresponding to incubation times of 10 and 130 min, respectively. The binding values are expressed as a percentage of the maximal amount of labeled ligand binding which occurs in the absence of the nonlabeled inhibitor at the times indicated above. The concentration of the labeled ligand was either 0.08 nM (*A*, *C*) or 0.8 nM (*B*). The association rate constant of the labeled ligand (k_1) was always 1.03×10^9 M^{-1} min^{-1}. The dissociation rate constant of the labeled ligand (k_{-1}) was either 2.45×10^{-2} min^{-1} (*A*, *C*) or 2.45×10^{-1} min^{-1} (*B*). The association rate constant of the nonlabeled ligand (k_2) was assigned values of k_1 (*Ai*, *Bi*, *Ci*), $0.1k_1$ (*Aii*, *Bii*, *Cii*), and $10k_1$ (*Aiii*, *Biii*, *Ciii*). The dissociation rate constant of the nonlabeled ligand (k_{-2}) was assigned values of k_{-1} (*A*), $0.1k_{-1}$ (*B*), and $10k_{-1}$ (*C*).

curve shifted to the left as equilibrium was approached (Fig. 1, *Ai–Aiii*, *Bi–Biii*). These shifts in the competition curves were independent of the association rate constants. In contrast, when the dissociation rate constant of the nonlabeled drug was greater than that of the labeled drug, the competition curve shifted to the right as equilibrium was approached (Fig. 1, *Ci–Ciii*). Once again, the shift in the competition curve was independent of the association rate constants.

The accuracy of the numerical method was tested by comparing the equilibrium binding values shown in Fig. 1 with the binding values calculated by using the competitive inhibition equation, Eq. 5. For this comparison, the free concentration of the labeled drug was assigned a value equal to its concentration at the IC_{50} point of the competition curve. When this comparison was made, results accurate to three decimal places were obtained. Also, when the time increment ($t_{i+1} - t_i$) for solving the differential equations was reduced by a factor of 0.1, the same values were computed for all pre-equilibrium conditions.

The theoretical time course of the kinetics of competitive inhibition is shown in Fig. 2, which illustrates the inhibition of radiolabeled drug binding produced by a nonlabeled drug at its IC_{50} concentration. For this analysis, the association rate constants of the labeled and nonlabeled drugs were assigned equal values, whereas the dissociation rate constants varied. As shown in Fig. 2, when the dissociation rate constant of the nonlabeled drug was equal to or less than that of the labeled drug, the percentage inhibition of radiolabeled ligand binding increased as equilibrium was approached, whereas the converse was true for a nonlabeled drug having a larger dissociation rate constant.

Effect of incubation time on the competitive inhibition of [^{3}H]QNB and [^{3}H]CD binding. Figure 3 shows the effects of incubation time on the competitive inhibition of [^{3}H]QNB binding by atropine and oxotremorine. Increasing the incubation time from 10 to 60 min increased the IC_{50} values of atropine and oxotremorine from 3.0 nM and 2.8 μM to 16 nM and 13 μM, respectively. Thus, an apparent 5-fold reduction in the affinity of atropine and

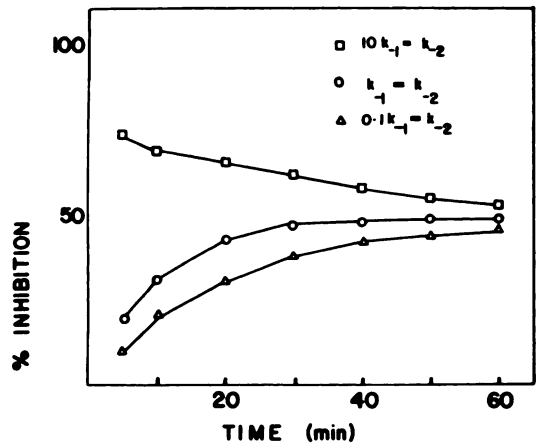

FIG. 2. *Effect of incubation time on the competitive inhibition of ^{3}H-labeled ligand binding by a nonlabeled inhibitor*

The percentage inhibition of ^{3}H-labeled ligand binding caused by a nonlabeled inhibitor at its IC_{50} concentration is plotted as a function of time. Theoretical binding values were computed numerically. For this analysis, the association rate constants (k_1, k_2) of the labeled ligand and nonlabeled competitive inhibitor were assigned the same value (1.03×10^9 M^{-1} min^{-1}). The dissociation rate constant of the labeled drug (k_{-1}) was either 2.45×10^{-2} min^{-1} (○, △) or 2.45×10^{-1} min^{-1} (□). The dissociation rate constant of the nonlabeled inhibitor (k_{-2}) was assigned values of k_{-1} (○), $0.1k_{-1}$ (△), and $10k_{-1}$ (□). The concentrations of nonlabeled inhibitor were 0.1 nM (○), 0.1 nM (△), and 1.0 nM (□).

oxotremorine occurred as the incubation time was extended. In contrast, the results of QNB/[^{3}H]QNB competitive inhibition experiments revealed a small reduction in the IC_{50} of QNB, from 1.3 to 0.80 nM, as the incubation time increased from 5 to 60 min (Fig. 4A). A similar time-dependent reduction in the QNB IC_{50} was seen in QNB/[^{3}H]CD competition experiments (Fig. 4B). In these studies, the IC_{50} of QNB decreased from 1.6 to 0.6 nM as the incubation time increased from 10 to 60 min.

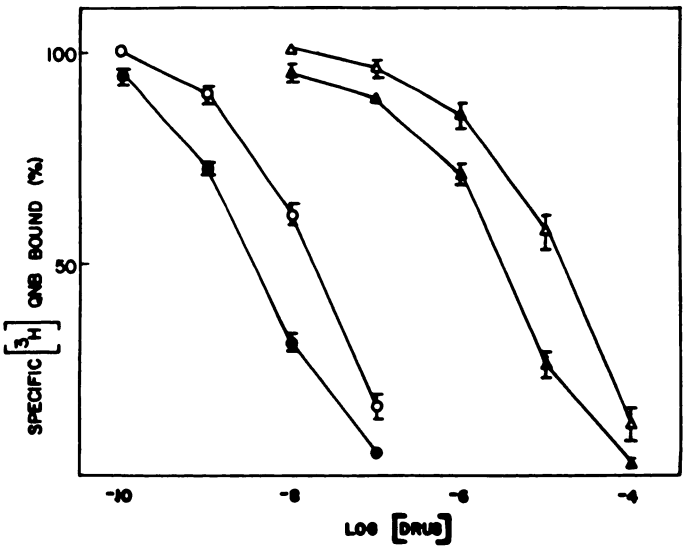

FIG. 3. *Effect of incubation time on the competitive inhibition of [^{3}H]QNB binding by atropine (○) and oxotremorine (△)*

Incubations were carried out for 10 min (●, ▲) and 60 min (○, △). Mean binding values ± standard error of the mean of four experiments are shown.

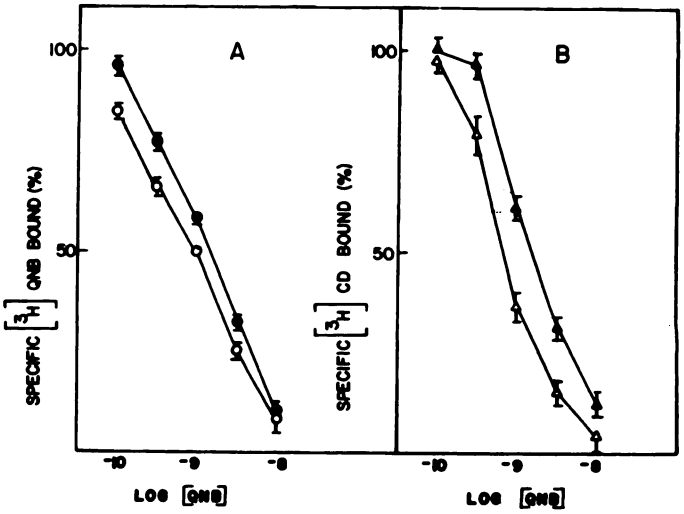

FIG. 4. *Effect of incubation time on the competitive inhibition of [^{3}H]QNB and [^{3}H]CD binding by QNB*

A. The competitive inhibition of [^{3}H]QNB binding by QNB was determined after 5-min (●) and 60-min (○) incubations. Mean binding values ± standard error of the mean of four experiments are shown.

B. The competitive inhibition of [^{3}H]CD binding by QNB was determined after 10-min (▲) and 60-min (△) incubations. Mean binding values ± standard error of the mean of four experiments are shown.

DISCUSSION

In a study of the kinetics of competitive inhibition in radioligand assays, theoretical calculations and experimental results showed that a competitive inhibition curve shifts to the left as equilibrium is approached if the labeled and nonlabeled ligands are the same (4). The mathematical analysis in this report is consistent with these previous findings and also describes cases in which the two competing ligands have different affinities. Our numerical simulations, the results of which are dependent on the initial conditions of the calculations, suggested that the shift of a competition curve was dependent on the ratio of dissociation rate constants of the two competing ligands. When the dissociation rate constant of the labeled ligand was less than or equal to that of the competing ligand, the competition curve shifted to the left as equilibrium was approached whereas the converse was true when the dissociation rate constant of the nonlabeled ligand was greater than that of the labeled ligand. However, since we did not examine all possible combinations of initial conditions, we are unable to conclude whether the time-dependent shift of a competition curve is solely dependent on the ratio of dissociation rate constants of the two competing ligands. However, the agreement of the present numerical calculations with previous experimental results (10) and analytical results (5) supports the contention that the shift of a competition curve which occurs as equilibrium is approached is primarily dependent on the ratio of dissociation rate constants of the ligands.

In the present study, the results of the ligand/[^{3}H]-QNB and ligand/[^{3}H]CD competition experiments can be rationalized in terms of the rate constants of the competing ligands and the theoretical predictions described above. Binding studies (7, 9) have shown that the

affinities of atropine and oxotremorine are less than that of QNB, a property which is due most likely to the slow rate of dissociation of QNB as compared with the other compounds. The results of atropine and oxotremorine/[^{3}H]QNB competition experiments showed that the competition curve shifts to the right as equilibrium is approached, which is consistent with the kinetic analysis. In contrast, a small time-dependent shift to the left in the QNB/[^{3}H]QNB competition curve was observed which is also in agreement with the mathematical prediction for competition experiments involving the same labeled and nonlabeled ligands. In previous studies of the characterization of [^{3}H]CD binding (8, 11), we noted that the affinity of [^{3}H]CD for muscarinic receptors is much less than that of QNB, suggesting that the dissociation rate of CD is much faster than that of QNB. Indeed, we have found that addition of 10 μM atropine to a [^{3}H]CD binding assay which has already reached equilibrium causes complete inhibition of binding within 15 min.[4] The dissociation rate of [^{3}H]QNB has been shown to be much slower (7, 9). In agreement with the theoretical predictions for competition experiments involving a nonlabeled drug which has a smaller dissociation rate constant than that of the labeled drug, we observed a shift to the left in the QNB/[^{3}H]CD competition curve as equilibrium was approached.

It should be emphasized that the bimolecular interaction model used in the present study is a simplification of ligand interactions with neurotransmitter receptors. It is reasonable to assume that agonists induce a conformational change in the receptor, and thermodynamic evidence in support of agonist-isomerization of the *beta*-adrenergic receptor has been obtained (12). However, if the agonist-induced isomerization process is rapid with respect to the rate of ligand binding, kinetics consistent with a bimolecular interaction will occur. Also, evidence has accumulated which suggests that muscarinic antagonists induce a conformational change in muscarinic receptors (13–15). Thus, the theoretical competition curves shown in this study should be considered approximate as compared with a more realistic model which would account for ligand-receptor isomerization. However, the agreement of the experimental results with the theoretical predictions suggests that the kinetics of competitive inhibition can be described generally by a bimolecular process. The mathematical analysis of the kinetics of ligand-receptor isomerization has been described by Van Ginneken (2).

The results of the present study suggest caution in designing and interpreting competitive inhibition experiments. We have noticed that some investigators have measured the percentage inhibition of ^{3}H-labeled antagonist binding by a given concentration of an agonist at various incubation times as a method of detecting agonist-induced densensitization. The usual interpretation of the data is that a lack of a time-dependent change in the percentage inhibition of binding represents no change in agonist affinity, whereas a time-dependent reduction in the inhibition of binding is indicative of agonist-induced desensitization. The data in our study demonstrate that, if the dissociation rate constant of the agonist is greater than that of the ^{3}H-labeled antagonist, a time-dependent reduction in agonist inhibition of ^{3}H-labeled antagonist binding is completely consistent with the kinetics of competitive inhibition assuming no desensitization. Experimental results showing no change in the percentage inhibition of binding might be construed as evidence for a time-dependent enhancement of agonist affinity. In any case, the kinetics of competitive inhibition is complex, and the interpretation of these kinds of data should not rely heavily on intuitive notions.

[4] F. J. Ehlert, W. R. Roeske, and H. I. Yamamura, unpublished observations.

ACKNOWLEDGMENTS

The authors wish to thank Susan Yamamura for her expert appraisal of the manuscript. We also acknowledge the expert technical assistance of David Chapman and the excellent secretarial assistance of Cathleen Thomas and Isabelle Preiss.

REFERENCES

1. Hollenberg, M. D. Receptor models and the action of neurotransmitters and hormones, in *Neurotransmitter Receptor Binding* (H. I. Yamamura, S. J. Enna, and M. J. Kuhar, eds.) Raven Press, New York, 13–39 (1978).
2. Van Ginneken, C. A. M. Kinetics of drug-receptor interaction, in *Handbook of Experimental Pharmacology*, (J. M. Van Rossum, ed.), Vol. 47. Springer-Verlag, Berlin, Heidelberg, New York, 357–411 (1977).
3. Berson, S. A., and R. S. Yalow. Quantitative aspects of the reaction between insulin and insulin-binding antibody. *J. Clin. Invest.* **38**:1996–2016 (1959).
4. Rodbard, D., H. J. Ruder, J. Vaitukaitis, and H. S. Jacobs. Mathematical analysis of kinetics of radioligand assays: improved sensitivity obtained by delayed addition of labeled antigen. *J. Clin. Endocrinol. Metab.* **33**:343–355 (1971).
5. Aranyi, P., Kinetics of the hormone-receptor interaction: competition experiments with slowly equilibrating ligands. *Biochim. Biophys. Acta* **628**:220–227 (1980).
6. Stark, P. A. Ordinary differential equations, in *Introduction to Numerical Methods*. Macmillan, New York, 235–272 (1970).
7. Yamamura, H. I., and S. H. Snyder. Muscarinic cholinergic binding in rat brain. *Proc. Natl. Acad. Sci. U. S. A.* **71**:1725–1729 (1974).
8. Ehlert, F. J., Y. Dumont, W. R. Roeske, and H. I. Yamamura. Muscarinic receptor binding in rat brain using the agonist, [^{3}H]cis-methyldioxolane. *Life Sci.* **26**:961–967 (1980).
9. Fields, J. Z., W. R. Roeske, E. Morkin, and H. I. Yamamura. Cardiac muscarinic cholinergic receptors. *J. Biol. Chem.* **253**:3251–3258 (1978).
10. Bouton, N. M., and J. P. Raynaud. The relevance of kinetic parameters in the determination of specific binding to the estrogen receptor. *J. Steroid Biochem.* **9**:9–15 (1978).
11. Ehlert, F. J., W. R. Roeske, and H. I. Yamamura. Regulation of muscarinic receptor binding by guanine nucleotides and N-ethylmaleimide. *J. Supramol. Struct.* (in press).
12. Weiland, G. A., K. P. Minneman, and P. B. Molinoff. Fundamental difference between the molecular interactions of agonists and antagonists with the β-adrenergic receptor. *Nature (Lond.)* **281**:114–117 (1979).
13. Galper, J. B., and T. W. Smith. Properties of muscarinic acetylcholine receptors in heart cell cultures. *Proc. Natl. Acad. Sci. U. S. A.* **75**:5831–5835 (1978).
14. Kloog, Y., Y. Egozi, and M. Sokolovsky. Characterization of muscarinic acetylcholine receptors from mouse brain: evidence for regional heterogeneity and isomerization. *Mol. Pharmacol.* **15**:545–558 (1979).
15. Jarv, J., B. Hedlund, and T. Bartfai. Kinetic studies on muscarinic antagonist-agonist competition. *J. Biol. Chem.* **255**:2649–2651 (1980).

Send reprint requests to: Dr. Henry I. Yamamura, Department of Pharmacology, University of Arizona Health Sciences Center, Tucson, Ariz. 85724.